

# Discovering equations from data: symbolic regression in dynamical systems

Beatriz R. Brum\* and Luiza Lober†

*Institute of Sciences Mathematics and Computation,  
Universidade de São Paulo-Campus de São Carlos,  
Caixa Postal 668, 13560-970 São Carlos, São Paulo, Brazil*

Isolde Previdelli

*Statistic Department, State University of Maringá, Maringá, Brazil.*

Francisco A. Rodrigues

*Department of Mathematics Applied and Statistics,  
Institute of Sciences Mathematics and Computation,  
Universidade de São Paulo-Campus de São Carlos,  
Caixa Postal 668, 13560-970 São Carlos, São Paulo, Brazil*

The process of discovering equations from data lies at the heart of physics and in many other areas of research, including mathematical ecology and epidemiology. Recently, machine learning methods known as symbolic regression have automated this process. As several methods are available in the literature, it is important to compare them, particularly for dynamic systems that describe complex phenomena. In this paper, five symbolic regression methods were used for recovering equations from nine dynamical processes, including chaotic dynamics and epidemic models, with the PySR method proving to be the most suitable for inferring equations. Benchmark results demonstrate its high predictive power and accuracy, with some estimates being indistinguishable from the original analytical forms. These results highlight the potential of symbolic regression as a robust tool for inferring and modelling real-world phenomena.

**Keywords:** Symbolic regression, Dynamic processes, Data driven approaches.

## I. INTRODUCTION

The discovery of equations from observational data is one of the fundamental pillars of the traditional scientific method. From the work of Johannes Kepler, who inferred the laws of planetary motion from meticulous astronomical observations [1] collected by Tycho Brahe [2], to Isaac Newton's theoretical formulations that consolidated classical mechanics, the process of identifying mathematical relationships underlying natural phenomena has historically been characterized by its manual nature, based essentially on systematic trial-and-error procedures.

However, in recent decades, the advent of Big Data, characterized by the production of an immense volume of complex, mostly nonlinear, data, in several fields has driven a new search for physical laws. Faced with the need to analyze these data sets to understand their intrinsic structure and derive symbolic representations that capture the integral behavior of a system, the demand for advanced analytical methods has become growing and indispensable.

With the emergence of modern computational techniques, this process has undergone a radical transformation, driving the widespread development and use of various regression techniques. In this context, symbolic regression (SR) emerges as a powerful tool to automate the

discovery of mathematical expressions underlying data. Unlike parametric methods, which are limited to adjusting coefficients in predefined equations and require extensive analysis of statistical significance, goodness-of-fit, and model diagnostics, SR simultaneously searches for the structure of the equation and its parameters. This search is performed by exploring a vast combinatorial space composed of mathematical operators, variables, and constants, which gives SR greater efficiency in modeling complex relationships.

Using a diverse set of techniques from the field of artificial intelligence, symbolic regression models can base themselves on genetic algorithms [3], sparse regression [4, 5], neural networks [6] and Kolmogorov-Arnold representations [7, 8]. Most of these are originally conventional algorithms that make no prior assumptions about the model structure [9], limiting human interaction to the definition of basic parameters to execute the algorithm. In contrast, more recent models allow for more substantive interaction between the user and the machine. In these unconventional approaches, in addition to configuring fundamental parameters, it is possible to incorporate prior knowledge about the dynamics that generate the data, an assumption that guides the algorithm in the search for the desired symbolic expression.

In this study, symbolic regression was applied to data from different dynamic systems. The objective was to derive the mathematical expressions that govern each dynamic, and in some cases this was done in a semi-supervised manner. This hybrid approach was chosen to avoid underestimating the capacity of certain SR al-

---

\* beatrizbrum@usp.br

† luiza.lober@usp.br

gorithms, a bias that could compromise the inference of the study results due to its unconventional nature.

The proposed method for analyzing these systems showed that certain algorithms can recover the structural form of specific dynamics with high accuracy. This result paves a way for this method to be used in real world data in future studies.

### A. Symbolic regression

The first supervised learning method capable of inferring governing equations from data was introduced by Langley [10], resulting in the BACON algorithm. However, this framework struggled with equations involving constraints, performed poorly with noisy data, and was limited by the modest computing power available in the 1970s. These challenges caused the idea of automating equation discovery to be largely set aside for several decades.

A few years later, in 1975, John Holland and his colleagues at the University of Michigan introduced the concept of genetic algorithms (GAs) [11]. Inspired by the principles of natural selection [12], GAs provide a framework for optimizing parameters through evolutionary processes. Building on this idea, Koza [13] introduced genetic programming (GP), which represents candidate solutions as decision trees and iteratively evolves them to discover governing equations for dynamical systems [14]. These advances created the foundation for symbolic regression, offering a systematic approach to extract mathematical relationships directly from observational data, as illustrated in Figure 1.

In recent years, symbolic regression algorithms have gained prominence as they focus on optimization and exploration of approximate solutions for systems with unknown equations of motion [15]. Building on the principles of symbolic regression, dissimilarity analysis, and mating strategies, Gustafson *et al.* [16] enhanced genetic programming, achieving overall improvements in solution accuracy that were validated through statistical tests.

Later, Schmidt and Lipson [17] developed a method known as Pareto GP which is augmented by Pareto optimization. Experimental data was collected from computationally tracked motion, which was then used by the model to find the governing equations of that system through either characteristic Lagrangians or Hamiltonians.

The process of searching in the space of symbolic expressions was accelerated by another contribution of genetic programming, where simpler models were used as a basis towards more complex representations. Another algorithm that benefits from this approach is the *Eureqa*, focusing not only in the search for a single symbolic expression, but rather the set of optimal expressions according to their complexity. An evaluation of this algorithm's performance can be seen in [18].

In this context of evolutionary algorithms, [3] proposed

GPlearn, an open source algorithm written in the Python programming language and using the *scikit-learn* library as its base, enabling the integration of this method with other popular machine learning techniques.

It is also worth mentioning that, parallel to the contributions made by genetic programming, [5] combined sparsity-promoting techniques and machine learning with dynamic systems to discover governing equations from noisy data. This methodology allowed the proposed algorithm to be used both in simple and in high-dimensional systems. For instance, it has several applications in both linear and nonlinear oscillatory dynamics, such as chaotic Lorenz systems and fluid vortex shedding behind an obstacle [5].

Also drawing from sparsity-based algorithms, [19] developed an algorithm for implicit ordinary differential equations (implicit-SINDy), a contribution to discover dynamic systems in metabolic and regulatory networks, which often exhibit nonlinear dynamics with rational function nonlinearities in their formulation. This algorithm can be applied to biological networks such as Michaelis-Menten enzyme kinetics, a regulatory network in bacteria and the metabolic network for yeast glycolysis.

Still in the same group of sparsity-promoting techniques, [20] developed a method capable of discovering partial differential equations based on time series measurements, which is a technique that can identify more complex and nonlinear dynamic models.

Exploring the proposal by [21] for the relaxed sparse regularized regression, or SINDy-SR3, [22] presented a sparse optimization framework capable of learning parsimonious models of dynamic systems from data, a formulation that aims to discover the equations of a dynamic system through data and by selecting relevant terms from an array of possible functions. This proposal of a comprehensive framework of symbolic regression models, driven by time series data, resulted in the “sparse identification of non linear dynamics” regression package in Python, also known as PySINDy, which also encompasses various optimizers and necessary tools for the functioning of the algorithm. [4, 5, 23, 24].

Symbolic regression can also benefit from neural network architectures, as first demonstrated by Sahoo *et al.* [25]. In their work, a method applied to a cart-pendulum system leveraged a neural network framework to identify functional relationships and generalize them from observed data to previously unexplored regions of the parameter space.

Another contribution that combined neural networks with a set of physics-inspired techniques comes from [6], which proposed a multidimensional recursive symbolic regression algorithm known as AI-Feynman. The approach was validated by effectively discovering all of the 100 selected equations from Feynman's lectures on physics [26], and as a consequence was considered one of the best algorithms available to the investigation of physical systems, raising the interest in using symbolic regression

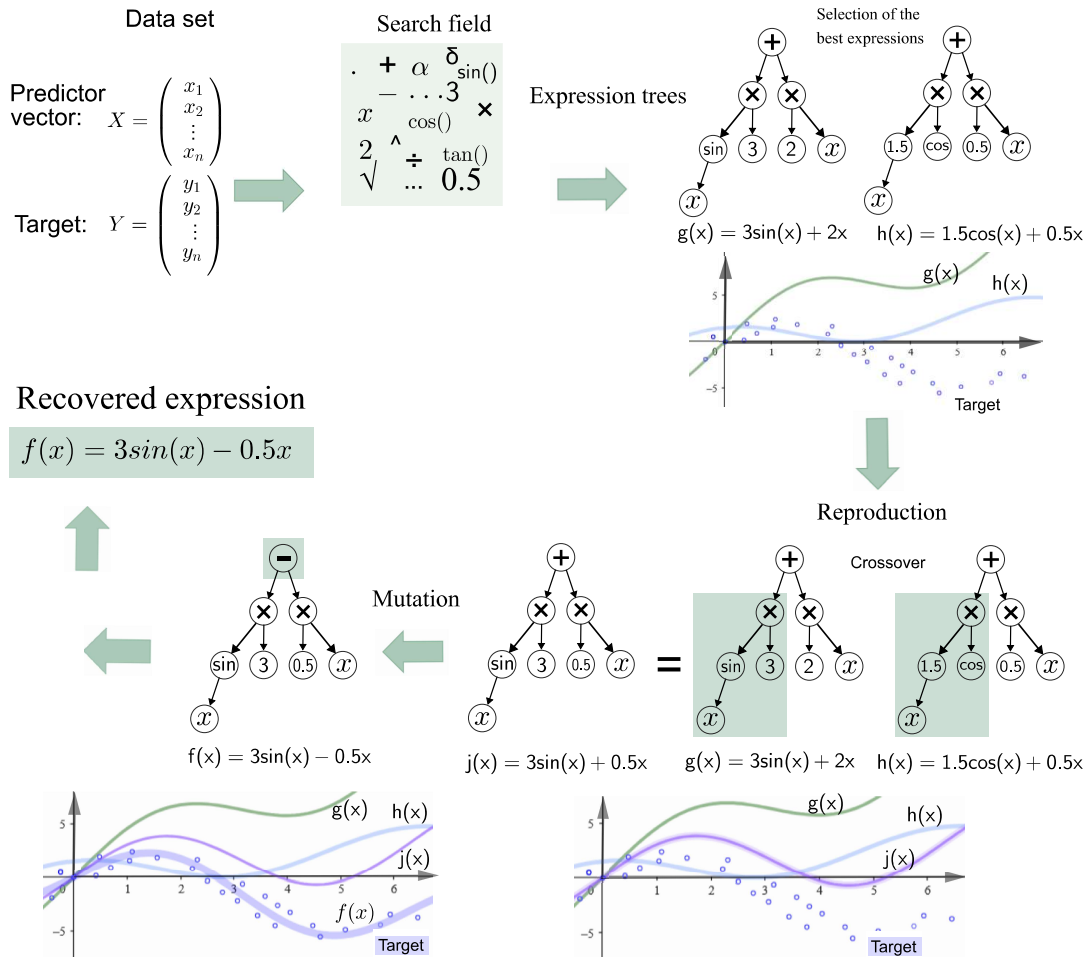


FIG. 1. Diagram of the usual process for adjusting a symbolic regression algorithm, using any model as an example of a possible application. They iterate new combinations of functions and increases in model complexity until they find the best fit. (\*) Mutation and crossover operators are only observed in algorithms based on genetic programming.

algorithms in this field.

The PyKAN method [7] offers an interesting alternative to the previously mentioned algorithms, drawing on the Kolmogorov–Arnold representation theorem within a neural network framework. Instead of relying on fixed activation functions as in traditional neural networks, Kolmogorov–Arnold networks use learnable univariate functions on the edges of the neural network, combined through multivariate linear operations at the nodes. This design provides both high expressivity and interpretability, making them well suited for symbolic regression tasks. Building on this foundation, several extensions have been proposed, such as the MultKAN model [8], which currently represents one of the most recent advancement in symbolic regression.

Most state-of-the-art symbolic regression algorithms still build on genetic programming. Among them, PySR, developed by Cranmer [27], stands out as a powerful tool for generating interpretable models. Implemented in Julia for high-performance computation, PySR is highly optimized while also providing a convenient Python in-

terface, making it both efficient and accessible to researchers.

## B. Symbolic regression algorithms

The symbolic regression models employed in this study are open-source algorithms that represent some of the most recent and significant contributions to the field, as discussed in the previous section. These include: (i) GPlearn, an evolutionary algorithm [3]; (ii) AI-Feynman, which combines neural networks with algebraic simplification techniques [6, 24]; (iii) PySINDy, based on sparse regression [23]; (iv) PySR, which leverages genetic programming [27]; and (v) PyKAN, a neural-network-based approach [7]. Each of these methods will be discussed in the following subsections.

### 1. *GPLearn*

The algorithm GPLearn is based on genetic programming and starts its search by randomly generating a population of symbolic expressions. These expressions are the result of combinations from the search space, which is composed of operators and functions defined by the user, such as  $\{+, -, *, \sin, \dots\}$ . These combinations generate several symbolic expressions, each containing a single genetic code represented by a uniquely coded chromosome.

The evaluation of each individual fit,  $f(\mathbf{x})$ , is performed through transformations, i.e., the mappings of genotype-phenotype ( $f_g$ ) and phenotype-fitness ( $f_p$ ) [28], where the resulting convolution  $f = f_p(f_g(\mathbf{x}^g))$  is determined. Based on goodness of fit, concepts analogue to those proposed by Darwin are utilized, where the fittest individuals are selected to keep evolving while the others are eliminated [15]. Now with a new and smaller population, these individuals undergo a selection process in pairs. Next comes reproduction, based on the fundamental principles of genetic inheritance theories developed by Mendel in 1865. At this stage, the algorithm performs crossovers and mutations, generating a new population that will be subjected to the entire process again until convergence occurs and the desired expression is found.

### 2. *AI-Feynman*

The AI-Feynman algorithm, developed at MIT's Artificial Intelligence Laboratory, is one of the most widely recognized symbolic regression methods due to its strong descriptive power in physics, as discussed in section IA. A key strength of this algorithm lies in the similarity between its procedure and the way physicists traditionally model phenomena. This explains its effectiveness in the physical sciences, where expressions are often compositional – that is, a function  $f$  can typically be represented as a combination of a small set of elementary functions (e.g., through linear combinations or other structured compositions). The AI-Feynman algorithm mirrors this process, which underpins its success in uncovering governing equations in physics.

The set of tools employed by this method ranges from simple processes in the search for symbolic representations, to the application of state-of-the-art machine learning techniques, with the resulting expression being generated through a tree encoding using reverse Polish notation [6]. The algorithm has been enhanced through methods that exploit common simplifying properties in natural physical processes, such as dimensional analysis, a straightforward approach resulting in a considerable reduction of the initial variable space, solving the issue of overshooting the complexity necessary for the expressions.

Additionally, it also includes nonlinear least squares polynomial fitting, allowing for the adjustment of polynomials ranging from zero to the fourth degree. The

method also uses an exhaustive search algorithm, generating a space that includes all possible expressions, from the simplest to the most complex with varied parameter combinations. Moreover, fitting can also be done using neural network-based structures, also simplifying the investigation of symmetry and separability properties. Finally, equality checking and data transformations are also accommodated by the algorithm. These features are considered the main strength of AI-Feynman since they allow for enough versatility to accurately describe physical laws.

### 3. *PySINDy*

PySINDy algorithm adopts a sparse regression constraint in its formulation to identify nonlinear differential equations. This technique also penalizes the error function and facilitate the identification of coefficients with nonlinear behavior by weighting terms according to a set criteria. The structural form of the aforementioned sparse formulation can be expressed as

$$\frac{d}{dt}x(t) = f(\mathbf{x}(t)). \quad (1)$$

The dynamics in  $f$  is required to be sparse in the state variables  $\mathbf{x}(t) \in \mathbb{R}^n$  [29], while the derivative of each of the different variables tends to be sparse in the space of possible functions. For example, in the linear combination below,

$$f_i(x) = \xi_1\theta_1(x) + \xi_2\theta_2(x) + \dots + \xi_j\theta_j(x), \quad (2)$$

most of the coefficients will end up canceling each other out when an appropriate set of  $\theta_j$  functions are found.

The method then assumes an approximation of the form

$$\dot{\mathbf{X}} \approx \Theta(\mathbf{X})\Xi, \quad (3)$$

where  $\Xi$  is a set of coefficients that determines the active terms in  $f$ , which must satisfy the sparsity requirement in equation (3) [23, 24].

That results in the algorithm initializing with the following matrices:  $\mathbf{X}$  and  $\dot{\mathbf{X}}$ . The first one is composed of time series of the variables measured from the system. The second one corresponds to the target matrix of time derivatives, generated by differentiating  $\mathbf{X}$  through a set of differentiation methods available in the algorithm.

Next, the matrix  $\Theta(\mathbf{X})$  lists the candidate functions for the formulation of the sought symbolic expression. Through the regularization term  $R(\Xi)$ , used by the algorithm internally, restrictions are applied to the coefficients of the model's parameters, which characterizes the sparse regression. The parameter  $\lambda$  describes the threshold to assume sparsity, and to achieve that, the software also uses the Pareto curve algorithm, thus ensuring a more parsimonious model and avoiding overfitting.

#### 4. PySR

Based on genetic algorithms and implemented in Julia, PySR’s main advantage over the alternative GPLearn lies in the use of a framework with higher computational performance offered by this new programming language, while also standing out for its efficiency and robustness [27].

Furthermore, in the Julia environment, it is possible to implement custom functions in the code using SIMD kernels. These kernels can be applied at runtime, ensuring high performance by processing multiple operations on data simultaneously, performing automatic differentiation, and handling populations of mathematical expressions, while taking advantage of its optimization to parallel computing [27]. In the aforementioned paper, the concept of the “EmpiricalBench” was introduced, which is a tool designed to compare and evaluate different algorithms and measure the capabilities of symbolic regression in scientific applications.

Another interesting aspect of the algorithm is that executions with nested operators can be controlled, ensuring that undesired compositions between functions do not occur. It also allows for the implementation of unary operators based on theoretical knowledge about the data, as well as the display of the desired expressions in a user-friendly way.

#### 5. PyKAN

The core of PyKAN, which is a semi-supervised approach, was developed by Liu *et al.* [7], involves incorporating Kolmogorov-Arnold networks in place of multi-layer perceptron (MLP) neural networks in its structure. While MLPs are based on the universal approximation theorem, which specifies that it is possible to approximate continuous functions with arbitrary precision to accurately learn the data if these networks have an appropriate topology for that specific dataset. Achieving such a topology, however, is known to be a challenging task, and that also turns the model too specific to be applied to different problems.

In contrast, the Kolmogorov-Arnold representation theorem guarantees that every continuous function can be expressed as a combination of simpler functions. That is, given a set of variables derived from some defined physical process as a continuous function,  $f : [0, 1]^n \rightarrow \mathbb{R}$  can be represented as:

$$f(x_1, x_2, \dots, x_n) = \sum_{q=1}^{2n+1} \Phi_q \left( \sum_{p=1}^n \phi_{q,p}(x_p) \right), \quad (4)$$

where  $\Phi_q : [0, 1] \rightarrow \mathbb{R}$  e  $\phi_{q,p} : \mathbb{R} \rightarrow \mathbb{R}$  are continuous functions. This theorem serves as the theoretical foundation for Kolmogorov-Arnold networks [7]. The authors gen-

eralize the original representation, where the depth was 2 layers and the width was equal to  $2n + 1$  with  $n$  representing the number of input variables. The ability to introduce additional layers to these networks and train them using backpropagation allows for the discovery of more complex relationships typically encountered in real-world problems [7].

Kolmogorov-Arnold Networks (KANs) also differs from multi-layer perceptrons (MLPs) by not using fixed activation functions. Instead of conventional weights, KANs adopt one-dimensional functions along the edges, which are parameterized by splines during training. These splines are smooth functions that fit the data, allowing KANs to learn their own activation functions and providing greater flexibility in modeling.

The accuracy of KANs is remarkable due to their ability to avoid overfitting: when the network is fed with a training dataset, it learns a specific mapping. However, by using another part of the same dataset, the network learns a different mapping. In this way, it adjusts only a few control points, ensuring that previously learned information is retained. This is made possible by the control points of B-splines, which allow for local adaptation without compromising the knowledge already acquired, an often observed problem with MLPs. During the training stage of the KANs, it is possible to refine the spline grids, turning them denser and increasing the number of parameters, and as such allowing for more specialized models. Thus, KANs tend to adjust only a few nodes during training, preserving prior knowledge and incrementally adapting to new information.

The predominance of the multiplication operation in real physical systems motivated the authors to enhance the algorithm, leading to MultKAN’s release. As highlighted by Liu *et al.* [8], this new approach has the potential to reveal multiplicative structures present in data. Furthermore, the authors enriched the algorithm with tools that allow for the use of prior or empirical knowledge about the studied system, such as the KANCompiler, which provides a significant advantage in the search for symbolic expressions.

### C. Applications

The results from applying symbolic regression to multiple domains of knowledge can already be considered an overall positive contribution to science, with several examples to that coming from research done in the last decade. Among these contributions are the modeling of climate systems [30], as well as the search for hybrid algorithms in materials science [31]. For example, Chen *et al.* [32] employed the method to understand the dynamics of complex ecosystems, whereas Abdellaoui and Mehrkanoon [33] used symbolic regression modeling in wind speed prediction and Luo and Yu [34] applied them to understand the implied volatility surface in the financial market.

Additionally, Kiyani *et al.* [35] used GPlearn to discover unknown components of complex nonlinear PDEs using the domain decomposition approach, aiming to find the closed-form of an unknown nonlinear component. Gudetti *et al.* [36] demonstrated that SINDy can be used for NVH applications, with the objective of controlling and reducing the vibration in products, which is useful in automotive engineering and various other fields. Miyazaki *et al.* [37] employed AI-Feynman to discover the hyperbolic discounting model as a discount function that could not be solved previously. Wong and Cranmer [38] demonstrated that the use of symbolic regression with PySR can be adopted as an effective strategy to identify interpretable gravitational wave population models. Beyond the essence of these applications, there is still other areas that can benefit from this approach, such as epidemic modeling, acoustics and many others.

Depending on the context in which the data were produced, certain symbolic regression models may be more effective than the other symbolic regression alternatives, as demonstrated by the papers mentioned previously, and mapping becomes crucial for inference accuracy. Highly impactful works have presented increasingly accurate methods for regression tasks. However, there are still no standardized tests to evaluate their efficiency, due to the diversity and complexity in which each symbolic regression model was developed. Some proposed solutions to this problem are discussed below.

Udrescu and Tegmark [6], in the pursuit of cutting-edge technology, also developed a throughout comparison between their algorithm, AI-Feynman, and Eureqa [39], employing 120 synthetic datasets for this comparative analysis. La Cava *et al.* [40] introduced a benchmarking platform to evaluate the performance of 14 contemporary symbolic regression methods on 252 datasets, comparing them with 7 machine learning methods. The authors created SRBench to be a reproducible and open-source benchmarking project. Their work assessed the performance of the regression model and its ability to learn equations and simple systems.

Although extensive benchmarks of several symbolic regression algorithms was already performed by the aforementioned studies, not all the state-of-the-art models, such as PySR, are included in their evaluation. To better understand the capacity of these methods to recover governing equations, here we benchmark selected dynamic systems, including the still relatively unexplored use of symbolic regression models to analyze state changes to the spread of infectious diseases in compartmental epidemiological models. These systems, alongside others of interest, will be presented in the following section.

#### D. Dynamical systems

In this section, the four types of dynamic systems chosen to compare the algorithms described in section I A will be discussed. The fourth category of dynamic sys-

tems is comprised of another six systems, describing epidemic propagation through different assumptions on its composing compartments.

The dynamics presented in Sections ID 1 to ID 3 were chosen for their overarching relevance in the domains of physics and biology, allowing this study to analyze the performance of the symbolic regression algorithms in describing a chaotic system, predator and prey dynamics and oscillatory motion, this way anchoring the novel use of symbolic regression algorithms to epidemic models being proposed here to the overall performance of those methods in multiple fields.

##### 1. Lorenz attractor

A classic example of chaotic dynamics that originates from a model to atmospheric convection [41], and independently from single-mode laser dynamics [42], is given by the Lorenz-Haken equations, which are described by

$$\begin{aligned}\dot{x} &= \sigma(y - x) \\ \dot{y} &= -x(\rho - z) - y, \\ \dot{z} &= xy - \beta z\end{aligned}\quad (5)$$

where, considering Lorenz's derivation for the atmosphere,  $x$  is proportional to the rate of convection of a fluid,  $y$  the horizontal temperature variation and  $z$  is the vertical temperature variation.  $\sigma$ ,  $\rho$  and  $\beta$  are constants that relate to properties of that physical system. The system also appears in many other fields and have generalizations to higher dimensions [43].

##### 2. The non-linear pendulum

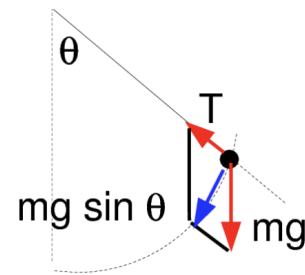


FIG. 2. Force diagram of the unitary non-linear pendulum.

Acquiring the equations of motion of this system analytically is relatively simple. To start, drawing the force diagram as done in Figure 2 already implies that the sum of forces will be  $F = mgsin(\theta)$ . Using Newton's second law of motion and taking  $x = r\theta = L\theta$ , the previous equation then becomes

$$F = m\ddot{x} = mL\ddot{\theta} = -mgsin\theta.$$

Noting that the angular frequency in this case is  $\omega = \sqrt{g/L}$  and  $\ddot{\theta} + F(\theta) = \ddot{\theta} + \omega^2 \sin \theta = 0$ , then by rewriting these terms, one arrives at the following equation:

$$\ddot{\theta} = -\frac{g}{l} \sin \theta \quad (6)$$

which, alongside  $u = \dot{\theta}$ , can then be used to simulate the behavior of this system.

### 3. Lotka-Volterra predator-prey dynamics

An essential baseline model in ecology, the Lotka-Volterra equations are used to simulate and understand the interaction of predator and prey populations in a food chain [44].

Even when making simplistic assumptions on the environment and the populations of the two interacting species, such as ample food being available at all times and that being entirely reliant on the prey population size, no account of genetic variation and adaptation, alongside of no environment changes, the model still is able to capture the general oscillations of population sizes that are observed in nature.

The system of equations that describe this model is given by

$$\begin{aligned} \dot{u} &= \alpha u - \beta u v \\ \dot{v} &= -\gamma v + \delta u v, \end{aligned} \quad (7)$$

where  $u$  represents the population density of prey,  $v$  the predator's.  $\alpha, \beta, \gamma, \delta \in \mathbb{R}^+$ , with  $\alpha$  as the maximum growth rate of prey per capita,  $\beta$  the effect of predators in the death rate of prey and, complementary to the last two,  $\gamma$  is the predator's per capita death rate and  $\delta$  the effect of prey in predator's growth rate.

When considering the equilibrium of the two populations, that is,  $u = \gamma/\delta$  and  $v = \alpha/\beta$  respectively for the prey and predator [45], both depend on each other's parameters, which as a consequence means that increasing the prey growth rate benefits the predator, with that in turn not granting an improvement to the prey population in the long term.

### 4. Epidemiological compartmental models

When studying the propagation of diseases in a population, a first step to understand the overall evolution of patients in a group is to compartmentalize each stage of the infection. In doing so, one can not only categorize populations, but also describe rates of transition from each category.

The simplest model that can be constructed that way considers only two states: susceptible (S) and infected (I) individuals. Assuming  $\beta$  as the infection rate,  $\gamma$  the

recovery rate and  $N$  the number of individuals, the resulting dynamics will be

$$\dot{I} = -\dot{S} = \frac{\beta}{N} IS - \gamma I \quad (8)$$

where it is assumed that no new individuals enter the group or leave it, or  $S(t) + I(t) = N$ .

If the individuals are allowed to recover from that disease, then  $R$  will be the total number of those that were cured, resulting in the following set of equations:

$$\begin{aligned} \dot{S} &= -\frac{\beta IS}{N} \\ \dot{I} &= \frac{\beta IS}{N} - \gamma I \\ \dot{R} &= \gamma I. \end{aligned} \quad (9)$$

In both cases, the parameters  $\beta$  and  $\gamma$  are essential to characterize the dynamics, as the basic reproductive number  $R_0 = \frac{\beta}{\gamma}$  is reliant on them, and characteristic of the disease's threshold: if each infected individual infects more than one susceptible individual, or  $R_0 > 0$ , then there's the onset of the epidemic. Otherwise, if  $R_0 < 0$ , the disease eventually vanishes from the population.

Expanding further from the aforementioned SIR and SIS systems, several other compartmental models can be built using other possible states for the individuals in a network. In this study, the following ones are used, with their equations shown in Table I (see also figure 3).

- SEIR [46], adding an exposed (E) category to the standard SIR;
- SEIRD [47], expanding the SEIR model by adding a deceased (D) count;
- SIRV [48], which vaccinated (V) individuals are also accounted for in the dynamics;
- SIRS [49], allowing reinfection in the SIR model.

Investigating several of these systems allows for broader conclusions on the efficiency of the symbolic regression algorithms examined, as these expanded compartmental models aim to account for the various phases and potential developments of an epidemic, drawing closer to real world disease spreading.

## II. METHODOLOGY

### A. Generating synthetic data

To accurately compare the five symbolic regression methods described in section IB, data from the dynamic systems described in section ID were generated to verify the ability of each symbolic regression model to identify the governing equations of those systems. All relevant

TABLE I. All compartmental models used and their governing equations, with transition rates as indicated in Figure 3.

| SIS   | SIR  | SEIR   | SEIRD  | SIRV  | SIRS   |
|---|--|--|--|---|--|
| $\dot{I} = -\dot{S} = \frac{\beta}{N}IS - \gamma I$<br>$\dot{S} = -\frac{\beta IS}{N}$<br>$\dot{I} = \frac{\beta IS}{N} - \gamma I$<br>$\dot{R} = \gamma I$ | $\dot{S} = -\frac{\beta IS}{N}$<br>$\dot{I} = \frac{\beta IS}{N} - \gamma I$<br>$\dot{R} = \gamma I$ | $\dot{S} = -\frac{\beta IS}{N} - \lambda S$<br>$\dot{E} = \frac{\beta IS}{N} - (\sigma + \gamma)E$<br>$\dot{I} = \sigma E - (\beta + \gamma)I$<br>$\dot{R} = \gamma I$ | $\dot{S} = -\frac{\beta SI}{N}$<br>$\dot{E} = \frac{\beta SI}{N} - \sigma E$<br>$\dot{I} = \sigma E - \gamma I$<br>$\dot{R} = \gamma(1 - \mu)I$<br>$\dot{D} = \gamma\mu I$ | $\dot{S} = -\frac{\beta SI}{N} - \epsilon S$<br>$\dot{I} = \frac{\beta SI}{N} - \gamma I$<br>$\dot{R} = \gamma I$<br>$\dot{V} = \epsilon S$ | $\dot{S} = -\frac{\beta SI}{N} + \delta R$<br>$\dot{I} = \frac{\beta SI}{N} - \gamma I$<br>$\dot{R} = \gamma I - \delta R$ |

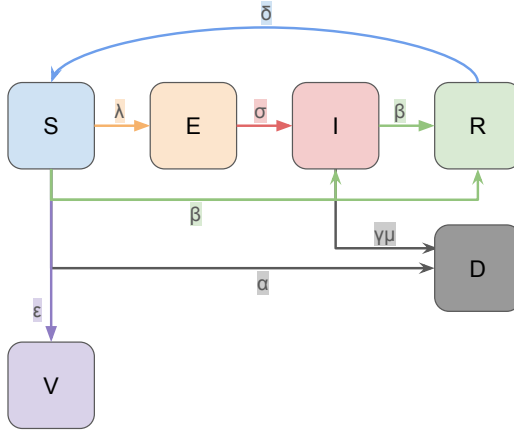


FIG. 3. Schematic of the compartmental transition for the selected epidemiological models, which use only parts of all compartments displayed. For their full equations, see Table I.

parameters chosen to generate this data on the dynamics are meant to exemplify the behavior of the given systems, and an exhaustive testing of parameter pairs and the resulting regression from the main methods applied to them are outside the scope of this study.

Tables VI and Table VIII appendix A present the parameters for the algorithms and initial conditions alongside intervals required for data simulations are provided, with the individual parameters for each systems' equations listed in Tables III and IV. The `SOLVE_IVP` function from the `SciPy` library was used to perform integration and solve the differential equations of each system.

### B. Metrics and definition of a baseline

To evaluate the performance of the chosen symbolic regression models, this study employed two methods, namely the comparison of structural forms of the original equations and the ones obtained by the symbolic regression algorithms, and integrating such equations over time to compare their evolution.

When ascertaining if the symbolic regression algorithms are indeed able to recover a given dynamic system's equations, an Wilcoxon signed-rank test [50] was employed to each and every regression performed, were it was assumed that no significant difference was observed for a system if  $\alpha = 0.05$  and  $p\text{-value} > 0.05$ .

As for assessing the efficacy of the symbolic regression

algorithms, while also anchoring them to other common place methods, a comparison of their performances with other machine learning models already established in the literature is necessary. To do so, the random forest [51] algorithm was employed, with the choice being justified due to its robustness recognizing patterns present in data from several fields, with those datasets also originating from large real-world systems [52].

Although frequently used for regression tasks, random forests and other tree-based algorithms do not provide interpretable equations like symbolic regression do, and as such this comparison is based on regression efficiency of this baseline model against the symbolic regression algorithms.

The adopted measurements to regression efficacy of the algorithms were based on two goodness of fit criteria: mean absolute error (MAE) and coefficient of determination ( $R^2$ ). The idea is to integrate both the original system's equations and the ones obtained by the symbolic regression algorithms in a given time frame and use these measurements to directly compare the differences in the evolution of the equations over time, if any.

## III. RESULTS AND DISCUSSIONS

Using the aforementioned parameters and applying the symbolic regression models to the datasets from Section II A, the results in Table III and IV were obtained. For all the following tables, dynamic systems whose structural forms were correctly identified, when compared to the original equations, are marked with a "check mark" (✓), while approximations or incorrect descriptions to these systems are left without those markings. The optimal parameters employed for each model can be found in the appendix on Tables VI and VIII.

Determining the structural form of the dynamics of a given system is a challenging task, also requiring fine tuning of the algorithms and quality data. Even so, Table II shows that all employed symbolic regression models demonstrated at least sufficient capability of identifying the symbolic representations of the several dynamic systems, specially when considering their effectiveness in the description of structural forms from epidemiological dynamics.

Table III shows that PySR was the top performing algorithms across the board, successfully identifying correct structural form of all systems, and six of them without significant difference, making this algorithm the most

TABLE II. Summary of the main results of Table III and Table I. Checkmarks indicates that the structural form of the system was successfully identified. The gray-shaded cells highlight the dynamics that showed no statistically significant differences compared to the original dynamics, according to the Wilcoxon test.

| Dynamic             | Symbolic Regression |            |         |      |       |
|---------------------|---------------------|------------|---------|------|-------|
|                     | GPLearn             | AI-Feynman | PySINDy | PySR | PyKAN |
| Lorenz              |                     |            | ✓       | ✓    | ✓     |
| Non-linear pendulum | ✓                   | ✓          | ✓       | ✓    | ✓     |
| Lotka-Volterra      | ✓                   | ✓          | ✓       | ✓    | ✓     |
| SIR                 | ✓                   | ✓          | ✓       | ✓    | ✓     |
| SIS                 |                     |            | ✓       | ✓    | ✓     |
| SEIR                |                     | ✓          |         | ✓    | ✓     |
| SEIRD               |                     |            |         | ✓    | ✓     |
| SIRV                | ✓                   | ✓          |         | ✓    | ✓     |
| SIRS                |                     |            |         | ✓    | ✓     |

versatile and accurate of all the ones tested.

The second best performing method was PyKAN, which also identified the equations of all systems correctly, however with fewer of them without significant differences. Although the semi-supervised method does produce worse results according to the metrics in Figure 4, it is more accurate when describing the equations of motion of a system. Moreover, the model proved to be more sensitive to the parameters used during the search: while stronger regularization favors the recovery of the approximate structural form, in some cases it appears to hinder parameter optimization.

AI-Feynman, also an semi-supervised method, was accurate with the description of five systems, only missing complete system identification by having significant differences on the Wilcoxon test for one system (Lotka-Volterra). Overall, the method only failed to recover the correct structural form of the chaotic Lorenz dynamics and the compartmental models SIS, SEIRD, and SIRS. However, it proved to be the most suitable for identifying the SEIR model, for which no statistically significant differences were detected. Together with PyKAN's result, this points to such methods having an use case when at least the main properties, constraints and parameters of the system are known, as these algorithms benefit greatly from prior, in-domain knowledge.

PySINDy also identified five systems, however not as accurately when considering the Wilcoxon's test results. Moreover, the method being quite accurate with the first five systems, but losing its effectiveness with more complex compartmental models can be explained by the decreasing sparsity in the data matrices of systems with more compartments, which in turn does not fulfill the necessary requirements for the model to correctly approximate a dynamic system, which would also likely be true for any other dynamic with more interacting parts.

Lastly, GPLearn missed most systems. Inspecting the resulting equations closely, one can see that beyond missing the values of a few parameters, its output equations are usually more complex than the original structural forms, featuring the multiplication and convolution of many terms, which is an usual feature used to

increase complexity in traditional genetic programming algorithms. GPLearn thus overshoots its results by not trimming the complexity of equations as other more recent genetic programming algorithms, such as PySR, are capable of doing.

Overall, although some of the resulting equations from the symbolic regression algorithms were only approximations to the real ones considered, the comparison to the originating physical and epidemic systems revealed that these differences were generally small, which can be verified when integrating the resulting equations in the same time frame as the original data and applying a modified MAE (see Figure 4 (a)) to calculate regression efficacy. This figure indicates that most algorithms can at least effectively capture the overall dynamics and provide an overview at the governing equations for varying phenomena.

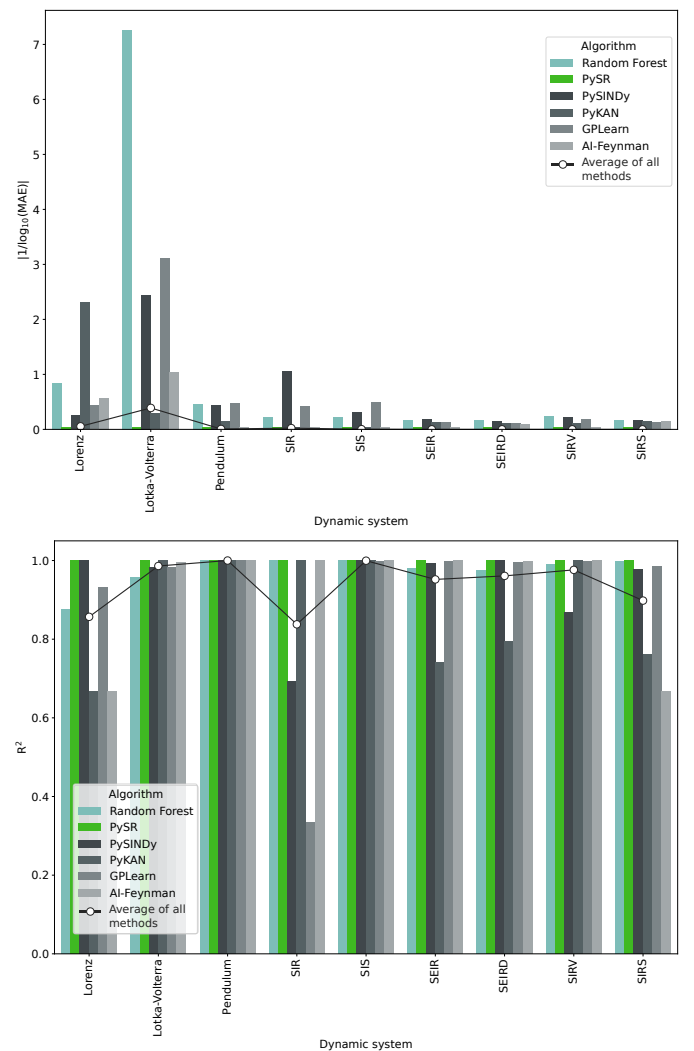


FIG. 4. The performance of the symbolic regression models for epidemiological simulations, evaluated in terms of (a)  $|1/\log(\text{MAE})|$ , with the black line displaying an average over all methods for a given dynamic and (b)  $R^2$ , with PyKAN values capped at -2 for better visualization.

#### IV. CONCLUSIONS AND OUTLOOK

This study provided a review of both the historic background of symbolic regression and state-of-the-art algorithms currently used by this emerging technique, while also benchmarking several of them in the task of recovering the governing equations of non-linear dynamics. Among all available symbolic regression algorithms, GPLearn, AI-Feynman, PySINDy, PySR, and PyKAN were selected for these detailed comparisons, using synthetic data of physical, biological and epidemiological systems, with the latter being an application still under-explored for these models. The methodology employed, along with the results obtained through it, allowed the identification of the best overall symbolic regression algorithms, while also presenting an efficient application of such techniques in a new domain.

PySR stood out as the most robust in discovering the dynamics to which it was applied, being able to identify the structural form of all of them, and only a few of those did not show a statistically significant difference compared to the original dynamics, although such differences in absolute values were small. Indeed, it is the most powerful in terms of recovering the underlying system structure from the data. PyKAN was also similarly capable, with only two dynamics presenting significant differences in comparison. This result helps bridge the gap in the current lacking benchmark both algorithms, although they still can benefit from being tested in other scenarios.

The AI-Feynman model also demonstrated high performance in identifying equations in the presented scenarios, finding expressions accurately for five out of nine systems, with only one (Lotka-Volterra) presenting significant differences from the originating system. However, it's important to mention that the algorithm's implementation, made available by the authors of the methodology themselves in [53], has not been maintained in a few years, with the last update dating from 2020. Future users of the code must be aware that technical difficulties may arise from the algorithm relying on dependencies that are out of date.

Other algorithms, namely GPLearn and PySINDy, had varying degrees of success, but did not perform well for the identification of epidemics that had more than three possible describing compartments, or the possibility of re-infection, with a single exception given by SIRV through GPLearn. The computational disadvantages of said models also points to them not being the best choice for such task.

The results of this study highlights the potential of symbolic regression, suggesting its possible consolidation as a new methodology for the modeling of data related to epidemic dynamics. This approach had not been thoroughly explored, and still has room to expand to real data from diseases already circulating. Moreover, updates to these algorithms or the development of new ones could bring even better performances to the already top per-

forming methods, overcoming current limitations and enabling more accurate dynamic recovery and better forecasting results in the future. The continuation of this study is essential to assess the capacity of these methods in describing dynamic systems and, consequently, their contribution to the description of epidemic spreading in real populations.

As for the current limitations of such approach, it is important to mention that even with the current advancements to this machine learning field, recovering equations from data through symbolic regression cannot be done in polynomial computational time, characterizing it as a NP-hard problem [54]. This should be taken into consideration when adding large sets of basis functions and their several permutations to these methods.

#### DATA AVAILABILITY

All relevant data to this review can be found in [55].

#### ACKNOWLEDGMENTS

Beatriz Brum thanks CAPES for the financial support provided (process number 33001014). Luiza Lober thanks São Paulo Research Foundation (FAPESP) through grants 2022/16065-3 and 2013/07375-0. Francisco A. Rodrigues acknowledges CNPq (grant 308162/2023-4) and FAPESP (grant 20/09835-1) for the financial support given for this research. This study was financed in part by the Coordenação de Aperfeiçoamento de Pessoal de Nível Superior – Brasil (CAPES) – Finance Code 001.

#### Appendix A: Tables with the parameters used to generate dynamic systems

The tables presented in this appendix specify the parameters used to generate the dataset employed in the article. The selection of these parameters was initially made randomly and then fine-tuned to each case. Table V outlines the parameters used in generating the systems described in Section II A on page 13. Table VII details the parameters utilized in constructing the data described in Section II.

TABLE III. Original structural form of the dynamic systems, alongside relevant parameters used by the dynamic systems to generate their synthetic data (first column), and equations found by each symbolic regression algorithm (all other columns). Dynamical systems whose structural forms were correctly identified are marked with “check mark” (✓).

| The sought expression   | GPLearn   | AI-Feynman  | PySINDy   | PySR   | PyKAN  |
|---|---|---|---|--|--|
| <b>Lorenz</b><br>$\dot{x} = 2(y - x)$<br>$\dot{y} = x(1 - z) - y$<br>$\dot{z} = xy - 2.6z$  | $\dot{x} = 2(y - x)$<br>$\dot{y} = x(1 - z) - y$<br>$\dot{z} = 0.19y - z$ | $\dot{x} = 2(y - x)$<br>$\dot{y} = x(1 - z) - y$<br>$\dot{z} = xy - 2.6z$ | $\dot{x} = 2.0(y - x)$<br>$\dot{y} = x(1 - z) - y$<br>$\dot{z} = xy - 0.6z$ | $\checkmark$<br>$\dot{x} = 2(y - x)$<br>$\dot{y} = x(1 - z) - y$<br>$\dot{z} = -xy - 2.6z$ | $\checkmark$<br>$\dot{x} = 2(y - x)$<br>$\dot{y} = x(1 - z) - y$<br>$\dot{z} = -xy - 2.6z$ |
| <b>Non linear pendulum</b><br>$\dot{\theta} = \omega$<br>$\dot{\omega} = -9.8 \sin(\theta)$ | $\dot{\theta} = \omega$<br>$\dot{\omega} = -9.17 * \sin(1.08 * \theta)$   | $\dot{\theta} = \omega$<br>$\dot{\omega} = -9.8 \sin(\theta)$             | $\dot{\theta} = \omega$<br>$\dot{\omega} = -9.8 \sin(\theta)$               | $\dot{\theta} = \omega$<br>$\dot{\omega} = -9.8 \sin(\theta)$                              | $\checkmark$<br>$\dot{\theta} = \omega$<br>$\dot{\omega} = -9.8 \sin(\theta)$              |
| <b>Lotka-Volterra</b><br>$\dot{u} = 2u - 0.5uv$<br>$\dot{v} = -v + 0.375uv$                 | $\dot{u} = 2u - 0.49uv$<br>$\dot{v} = -v + 0.37uv$                        | $\dot{u} = 2u - 0.5uv$<br>$\dot{v} = -0.99v + 0.33uv$                     | $\dot{u} = 1.94u - 0.49uv$<br>$\dot{v} = -0.95v + 0.37uv$                   | $\checkmark$<br>$\dot{u} = 2.0u - 0.5uv$<br>$\dot{v} = 0.37uv - 1.0v$                      | $\dot{u} = 2u - 0.5uv$<br>$\dot{v} = -v + 0.19uv$  |

TABLE IV. Description of the symbolic representations of the approximated epidemic propagation dynamics. Dynamical systems whose structural forms were correctly identified are marked with “check mark” (✓).

| Governing equation   | GPILearn   | AI-Feynman  | PySINDy   | PyKAN   |
|--|--|---|---|---|
| <b>SIR</b><br>$\dot{S} = -0.3SI$<br>$\dot{I} = 0.3SI - 0.1I$<br>$\dot{R} = 0.1I$                                     | ✓<br>$\dot{S} = -0.29SI$<br>$\dot{I} = 0.25SI - 0.08I$<br>$\dot{R} = 0.101I$   | ✓<br>$\dot{S} = -0.3SI$<br>$\dot{I} = 0.3SI - 0.1I$<br>$\dot{R} = 0.1I$   | ✓<br>$\dot{S} = -0.301SI$<br>$\dot{I} = 0.301SI - 0.1I$<br>$\dot{R} = 0.1I$   | ✓<br>$\dot{S} = -0.3SI$<br>$\dot{I} = 0.3SI - 0.1I$<br>$\dot{R} = 0.1I$   |
| <b>SIS</b><br>$\dot{S} = -0.3SI + 0.1I$<br>$\dot{I} = 0.3SI - 0.1I$<br>$\dot{R} = 0.1I$                              | ✓<br>$\dot{S} = -0.21S^2I$<br>$\dot{I} = 0.3SI - 0.102I$   | ✓<br>$\dot{S} = -0.2SI + 0.1I^2$<br>$\dot{I} = 0.25I - 0.1I^2$  | ✓<br>$\dot{S} = -0.301SI + 0.1I$<br>$\dot{I} = 0.301SI - 0.1I$  | ✓<br>$\dot{S} = -0.3SI + 0.1I$<br>$\dot{I} = 0.3SI - 0.1I$  |
| <b>SEIS</b><br>$\dot{S} = -0.3SI$<br>$\dot{E} = 0.3SI - 0.2E$<br>$\dot{I} = 0.2E - 1.0I$<br>$\dot{R} = 1.0I$         | ✓<br>$\dot{S} = -0.28SI$<br>$\dot{E} = S(-0.19E + 0.27I)$<br>$\dot{I} = 0.205E - I$<br>$\dot{R} = 1.0I$                              | ✓<br>$\dot{S} = -0.30SI$<br>$\dot{E} = 0.3SI - 0.2E$<br>$\dot{I} = 0.2E - I$<br>$\dot{R} = 1.0I$                          | ✓<br>$\dot{S} = 5.3I - 5.6SI$<br>$\dot{E} = -29.5E - 26.4I + 29.4SE + 26.7SI$<br>$\dot{I} = -1154.3E + 2709974.6I + 1156.0SE$<br>$\dot{R} = -2712688.329SI - 2744.1IE - 812252.0IR$   | ✓<br>$\dot{S} = -0.307SI$<br>$\dot{E} = 0.28SI - 0.28E$<br>$\dot{I} = 0.18E - 1.0I$<br>$\dot{R} = 1.0I$                             |
| <b>SEIR</b><br>$\dot{S} = -0.3SI$<br>$\dot{E} = 0.3SI - 0.2E$<br>$\dot{I} = 0.2E - (1.0 + 0.1)I$<br>$\dot{R} = 1.0I$ | ✓<br>$\dot{S} = -0.3SI$<br>$\dot{E} = -0.188SE - 0.306I(-S + E)$<br>$\dot{I} = 0.177E - I$<br>$\dot{R} = 1.0I$<br>$\dot{D} = 0.09I$  | ✓<br>$\dot{S} = -0.3SI$<br>$\dot{E} = -0.3SI - 0.1I$<br>$\dot{I} = 0.2E - 0.13I$<br>$\dot{R} = 1.0I$<br>$\dot{D} = 0.05I$ | ✓<br>$\dot{S} = 7.130I + -7.438SI$<br>$\dot{E} = -50.0E - 35.0I + 49.9SE + 35.3SI$<br>$\dot{I} = -1371.549E + 3056212.8I + 1373.4SE -$<br>$\dot{R} = -22.7I + 23.7SI$<br>$\dot{D} = -2.2I + 2.377SI$  | ✓<br>$\dot{S} = -0.3SI$<br>$\dot{E} = 0.3SI - 0.2E$<br>$\dot{I} = 0.196E - (1.0 + 0.08)I$<br>$\dot{R} = 1.02I$<br>$\dot{D} = 0.08I$ |
| <b>SIRV</b><br>$\dot{S} = -0.5SI - 0.5S$<br>$\dot{I} = 0.5SI - 1.0I$<br>$\dot{R} = 1.0I$<br>$\dot{V} = 0.5S$         | ✓<br>$\dot{S} = -SI - 0.495S$<br>$\dot{I} = 0.42SI - 0.89I$<br>$\dot{R} = 1.0I$<br>$\dot{V} = 0.48S$                                 | ✓<br>$\dot{S} = -0.5SI - 0.5S$<br>$\dot{I} = 0.5SI - 1.0I$<br>$\dot{R} = 1.0I$<br>$\dot{V} = 0.2S$                        | ✓<br>$\dot{S} = -2.2S + -5129152.8I - 8426634.8R - 20.2V$<br>$\dot{I} = 414.5I - 11175.8R - 0.034V$<br>$\dot{R} = -200.6I + 12367.7R + 0.03V + 201.8S * I$<br>$\dot{V} = 2.2S + 5108977.9I + 8392164.2R + 20.1V$<br>$\dot{R} = -5115878.2SI - 8405412.6S * R - 0.078SV - 1780761.03IR$<br>$\dot{V} = -5127836.9IV - 8418297.02RV$ | ✓<br>$\dot{S} = -0.49SI - 0.49S$<br>$\dot{I} = 0.5SI - 1.0I$<br>$\dot{R} = 1.0I$<br>$\dot{V} = 0.5S$                                |
| <b>SIRS</b><br>$\dot{S} = -0.3SI + 0.2R$<br>$\dot{I} = 0.3SI - 1.0I$<br>$\dot{R} = 1.0I - 0.2R$                      | ✓<br>$\dot{S} = -IR - 0.2I + 0.18R$<br>$\dot{I} = 0.28\left(\frac{(-\sqrt{(\sqrt{(S) + 1)}) + 1)}{I}\right)$<br>$\dot{R} = I - 0.2R$ | ✓<br>$\dot{S} = -0.3SI + 0.2R$<br>$\dot{I} = -0.71SI + 0.01I$<br>$\dot{R} = I - 0.25R$                                    | ✓<br>$\dot{S} = -3.3I + 0.4R + 3.0SI - 0.168SR$<br>$\dot{I} = -4.3I + 3.633SI$<br>$\dot{R} = 7.7I - 0.5R - 6.7SI + 0.3RS$   | ✓<br>$\dot{S} = -0.3SI + 0.2R$<br>$\dot{I} = 0.3SI - I$<br>$\dot{R} = 1.0I - 0.1R$  |

TABLE V. Initial conditions, parameters, data generation intervals and the time periods employed for solving the ODEs of interest (see II A) for the dynamics of Sections ID 1 to ID 3.

| Parameters           | Lorenz          | Nonlinear pendulum          | Lotka-Volterra |
|----------------------|-----------------|-----------------------------|----------------|
| Initial condition    | [0.6, 2.0, 1.0] | $[\omega = 0, \theta = 45]$ | [20, 5]        |
| Coefficients         | [2, 1.0, 2.6]   | [9.8, 1.0]                  | [2.0, 0.5, 1]  |
| Integration interval | [0,5]           | [0,5]                       | [0,7.5]        |
| Time increment       | 2E-3            | 2E-3                        | 1E-1           |

TABLE VI. Parameters employed by the SR algorithms to obtain a symbolic expression for a given system, which are the same as defined in Sec. II A.

| SR model | Parameters              | Dynamic System  |  |  |
|----------|-------------------------|---|--|--|
|          |                         | Lorenz  | Non-linear pendulum  | Lotka-Volterra   |
| GPLearn  | population_size         | 5000  | 5000   | 5000   |
|          | generations             | 50  | 100  | 50   |
|          | tournament_size         | 50  | 100  | 50   |
|          | stopping_criteria       | 0.01  | 0.01   | 0.01   |
|          | p_crossover             | 0.7   | 0.7  | 0.6  |
|          | p_subtree_mutation      | 0.2   | 0.2  | 0.2  |
|          | p_hoist_mutation        | 0.01  | 0.01   | 0.01   |
|          | p_point_mutation        | 0.09  | 0.09   | 0.09   |
|          | init_depth              | (2, 6)  | (2, 2)   | (8, 9)   |
|          | parsimony_coefficient   | 0.001   | 0.009  | 0.001  |
| PySINDy  | function_sett           | —   | $[\times, +, -, \div, \sin]$                                   | $[\times, +, -]$   |
|          | random_state            | 0   | 0  | 0  |
|          | library_functions       | Custom <sup>a</sup>   | Fourier (n_frequencies = 1)<br>Polynomial (degree=1)           | Polynomial (degree=3)  |
|          | feature_library         | $x, y, z$   | $\theta, \omega$   | $u, v$   |
|          | differentiation_method  | STLSQ   | FiniteDifference   | FiniteDifference (order=2)   |
|          | optimizer               | 0.2   | SR3  | SR3  |
|          | threshold               | 1E - 4  | 0.4  | 0.6  |
|          | alpha                   | False   | —  | 1E - 4   |
|          | normalize_columns       | —   | —  | True   |
|          | thresholder             | —   | 'l1'   | —  |
| PySR     | $\nu$                   | —   | —  | 1  |
|          | tol                     | —   | —  | 1E - 6   |
|          | Population              | [30, 30, 30]  | [1, 30]  |  |
|          | N iteration             | [30,30,30]  | [30,30]  | [10,50,800]  |
|          | Binary-Operator         | $[-, +, *], [-, +, *], [-, +, *]$   | $[*, +], [+,*]$  | $[*, +], [-, *]$   |
| PyKAN    | Unary-Operator          | $[[], [ ], [ ]]$  | $[[], "sin"]$  | $[[], [ ]]$  |
|          | Nested_constraints      | no  | no   | no   |
|          | Network topology        | $\begin{cases} x : \text{kanpiler} \\ y : \text{kanpiler} \\ z : \text{kanpiler} \end{cases}$ | $\begin{cases} \theta : [1, 1] \\ \omega : [1, 1] \end{cases}$ | $\begin{cases} U : \text{kanpiler} \\ V : \text{kanpiler} \end{cases}$ |
|          | seed                    | 0   | 12   | 0  |
|          | $\lambda$               | 1E-25   | 1E-3   | 1E-35  |
|          | steps                   | 50  | 30   | 60   |
|          | $\lambda_{\text{coef}}$ | 1E-19   | 1e-15  | 1E-2   |

<sup>a</sup> Customized function that excludes powers of x.

TABLE VII. Initial conditions, parameters, data generation intervals and the time periods employed for solving the ODEs of compartmental epidemic models (see ID 4).

| Parameters           | SIR               | SIS            | SEIR               | SEIRD                | SIRV                 | SIRS              |
|----------------------|-------------------|----------------|--------------------|----------------------|----------------------|-------------------|
| Initial condition    | [0.999, 0.001, 0] | [0.999, 0.001] | [0.999, 0.0001, 0] | [0.999, 0, 0.001, 0] | [0.999, 0, 0.001, 0] | [0.999, 0.001, 0] |
| Coefficients         | [0.3,0.1]         | [0.3,0.1]      | [0.3,0.2, 1.0]     | [0.5,0.5,1,0,0.1]    | [0.5,0.5, 1.0]       | [0.2,0.2, 1.0]    |
| Integration interval | [0, 100]          | [0,100]        | [0, 160]           | [0,100]              | [0,100]              | [0,100]           |
| Time increment       | 2E-3              | 2E-3           | 1                  | 5E-2                 | 5E-2                 | 5E-2              |

TABLE VIII. Parameters employed by each regression model and dataset, where each value refers to the parameter used for a certain compartment of the epidemic model, following the acronym's order. Time is measured in seconds.

| SR model   | Parameters              | Epidemiological models      |                      |                                       |  |  |  |
|------------|-------------------------|-----------------------------|----------------------|---------------------------------------|--|--|--|
|            |                         | SIR                         | SIS                  | SEIR                                  | SEIRD  | SIRV                                     | SIRS   |
| GPILearn   | population_size         | 10000                       | 5000                 | [1E4, 5E4, 1E4, 1E3]                  | [1E4, 6E4, 6E4, 2E3, 2E3]                      | [2E3, 6.5E2, 2E3, 2E3]                   | [1E4, 8E4, 1E4]                              |
|            | generations             | 100                         | 20                   | [2E3, 5E3, 2E3, 2E3]                  | [1E2, 6E3, 6E3, 3.5E2, 3.5E2]                  | [3.5E2, 5E2, 3.5E2, 3.5E2]               | [5E2, 1E3, 6E2]                              |
|            | tournament_size         | 100                         | 20                   | [2E3, 5E3, 2E3, 2E3]                  | [1E2, 6E3, -, 3.5E2, 3.5E2]                    | [3.5E2, 1.5E2, 3.5E2, 3.5E2]             | [5E2, 1E3, 5E2]                              |
|            | stopping_criteria       | 0.01                        | 0.01                 | [1E-2, 1E-3, 1E-4, 1E-2]              | [1E-3, 1E-2, 1E-2, 1E-3, 1E-3]                 | [1E-2, 1E-2, 1E-2, 1E-3]                 | 1E-2   |
|            | p_crossover             | 0.7                         | 0.6                  | 0.7                                   | [0.7,0.6,0.7,0.7,0.7]                          | 0.7                                      | 0.7  |
|            | p_subtree_mutation      | 0.1                         | 0.2                  | 0.1                                   | [0.1,0.2,0.2,0.1,0.1]                          | 0.1                                      | 0.1  |
|            | p_hoist_mutation        | 0.05                        | 0.01                 | [0.05, 0.05, 0.1, 0.1]                | [0.1,0.01,0.01,0.1,0.1]                        | 0.1                                      | 0.1  |
|            | p_point_mutation        | 0.1                         | 0.08                 | 0.1                                   | [0.1,0.09,0.09,0.1,0.1]                        | 0.1                                      | 0.1  |
|            | init_depth              | (3.6)                       | (2.3)                | [(2.5),(3.3),(2.3),(0.5)]             | [(2.2),(3.4),(2.3),(1.1),(1.1)]                | [(2.4),(3.3),(2.4)]                      | [(3.4),(3.3),(3.4)]                          |
|            | parsimony_coefficient   | 0.7                         | 0.01                 | [0.05, 0.001, 0.7, 0.05]              | [0.05, 0.01, 0.01, 0.01, 0.01]                 | 0.01                                     | 0.01   |
| AI-Feynman | function_sett           | [x, +]                      | [x, +, -, ÷]         | [None, [x, +], [x, +], [x, +]]        | [[x, -], [x, -], [x, -], [x, +, -], [x, +, -]] | [[x, -], [x, -], [x, -], [x, +], [x, +]] | [[x, -, -], [x, -, -], [x, -, -], [x, -, -]] |
|            | random_state            | 0                           | 0                    | 0                                     | 0  | 0  | 0  |
| PySINDY    | BF_try_time             | [60s, 60s, 60s]             | 60s                  | [240, 300, 3600, 60]                  | [3600, 60, 60, 60, 30]                         | [300,300,3600,60]                        | [3600,60,600]                                |
|            | BF_ops_file_type        | 7ops                        | 7ops                 | 7ops                                  | 7ops   | 7ops                                     | 7ops   |
|            | polyfit_deg             | 2                           | 2                    | 2                                     | [2.2,2.2,1]                                    | 2  | 2  |
|            | NN_epochs               | [400,400,4000]              | 400                  | [600,4000,600,600]                    | [1000,400,200,600, 600]                        | [4000,4000,600,1000]                     | [600,600,600]                                |
| PySR       | Function                | $x + y, x * y$              | $x + y, x * y$       | $x, x * y$                            | $x, x * y$                                     | $x, x * y$                               | $x, x * y$                                   |
|            | Optimizer               | STLSQ                       | STLSQ                | STLSQ                                 | OMP  | OMP                                      | STLSQ  |
|            | Threshold               | 0.6                         | 0.6                  | 1E-4                                  | no   | 1E-4                                     | 1E-3   |
|            | $\alpha$                | 1E-4                        | 1E-4                 | 1E-3                                  | no   | 1E-3                                     | 1E-4   |
|            | n_nonzero_coefs         | no                          | no                   | no                                    | 2  | 2  | no   |
| PyKAN      | Population              | [50,50,50]                  | [50,50]              | [50,50,50, 50]                        | [50,50,50,50]                                  | [50,50,50,50]                            | [50, 50, 50]                                 |
|            | model_selection         | "best"                      | "pest"               | "best"                                | "best"   | "best"                                   | "best"                                       |
|            | Paralelism              | "serial"                    | "serial"             | "serial"                              | "serial"                                       | "serial"                                 | "serial"                                     |
|            | Random_state            | 42                          | 42                   | 42                                    | 42   | 42                                       | 42   |
|            | deterministic           | "True"                      | "True"               | "True"                                | "True"   | "True"                                   | "True"                                       |
|            | Maxsize                 | 10                          | 10                   | 10                                    | 10   | 10                                       | 10   |
|            | niteration              | [1E3, 1E3,1E3]              | [1E3,1E3]            | [1E3,1E3,1E3,1E3]                     | [1E3,1E3,1E3,1E3]                              | [1E3,1E3,1E3,1E3]                        | [1E3,1E3,1E3]                                |
|            | Binary-Operator         | [+, *, -]                   | [+, *, -]            | [+, *, -]                             | [+, *, -]                                      | [+, *, -]                                | [+, *, -]                                    |
|            | Unary-Operator          | [[],[],[],[]]               | [[],[],[],[]]        | [[],[],[],[]]                         | [[],[],[],[]]                                  | [[],[],[],[]]                            | [[],[],[],[]]                                |
|            | Network topology        | [kanpiler, kanpiler, [1,1]] | [kanpiler, kanpiler] | [kanpiler, kanpiler, kanpiler, [1,1]] | [kanpiler, kanpiler, kanpiler, [1,1], [1,1]]   | [kanpiler, kanpiler, [1,1], [1,1]]       | [kanpiler, kanpiler, [2,1]]                  |
|            | seed                    | 0                           | 12                   | 0                                     | 0  | 12                                       | 12   |
|            | $\lambda$               | [1E-15, 1E-15, 1E-4]        | [1E-45,1E-25]        | [1.5E-5, 1, 1E-15, 1E-15]             | [1, 1, 1E-7, 1E-15, 1E-15]                     | [1E-3, 1E-3, 1E-15, 1E-15]               | [100, 1E-10, 1E-15]                          |
|            | steps                   | [50, 50,50]                 | [60,60]              | [50,50,50,50]                         | [70,70,50,50]                                  | [100,20,50,50]                           | [500,100,50]                                 |
|            | $\lambda_{\text{coef}}$ | [1E-5,1E-5,1E-3]            | [1E-2,1E-12]         | [150, 80, 1, 1]                       | [1E-2, 1E-2, 1E-15, 1, 1]                      | [1E-15, 1E-15, 1, 1]                     | [35,1,1]                                     |

---

[1] G. Camps-Valls, A. Gerhardus, U. Ninad, G. Varando, G. Martius, E. Balaguer-Ballester, R. Vinuesa, E. Diaz, L. Zanna, and J. Runge, Discovering causal relations and equations from data, arXiv preprint arXiv:2305.13341 (2023).

[2] M. Gleiser, *The dancing universe: From creation myths to the big bang* (UPNE, 2005).

[3] T. Stephens, Genetic programming in python, with a scikit-learn inspired api: gplearn (2016).

[4] S. L. Brunton, J. L. Proctor, and J. N. Kutz, Sparse identification of nonlinear dynamics with control (sindyc), IFAC-PapersOnLine **49**, 710 (2016).

[5] S. L. Brunton, J. L. Proctor, and J. N. Kutz, Discovering governing equations from data by sparse identification of nonlinear dynamical systems, Proceedings of the national academy of sciences **113**, 3932 (2016).

[6] S.-M. Udrescu and M. Tegmark, Ai feynman: A physics-inspired method for symbolic regression, Science Advances **6**, eaay2631 (2020).

[7] Z. Liu, Y. Wang, S. Vaidya, F. Ruehle, J. Halverson, M. Soljačić, T. Y. Hou, and M. Tegmark, KAN: Kolmogorov-Arnold Networks, arXiv 10.48550/arXiv.2404.19756 (2024), 2404.19756.

[8] Z. Liu, P. Ma, Y. Wang, W. Matusik, and M. Tegmark, Kan 2.0: Kolmogorov-arnold networks meet science, arXiv preprint arXiv:2408.10205 (2024).

[9] W. Minnebo and S. Stijven, *Empowering knowledge computing with variable selection-On variable importance and variable selection in regression random forests and symbolic regression*, Ph.D. thesis, Master's thesis, University of Antwerp, Antwerp, Belgium (2011).

[10] P. Langley, Bacon: A production system that discovers empirical laws., in *IJCAI* (Citeseer, 1977) p. 344.

[11] D. E. Goldberg, Genetic algorithms in search, optimization, and machine learning, Addison wesley **1989**, 36 (1989).

[12] C. Darwin, The origin of species by means of natural selection. popular impression of the corrected copyright edition (1910).

[13] J. R. Koza, Genetic programming, on the programming of computers by means of natural selection. a bradford book, MIT Press (1992).

[14] A. Diveev and E. Shmalko, *Machine Learning Control by Symbolic Regression* (Springer, 2021).

[15] S. Sivanandam and S. Deepa, *Introduction to genetic algorithms* (Springer, 2008) pp. 15–37.

[16] S. Gustafson, E. K. Burke, and N. Krasnogor, On improving genetic programming for symbolic regression, in *2005 IEEE Congress on Evolutionary Computation* (IEEE, 2005) pp. 02–05.

[17] M. Schmidt and H. Lipson, Distilling free-form natural laws from experimental data, science **324**, 81 (2009).

[18] R. Dubčáková, Eureqa: software review (2011).

[19] N. M. Mangan, S. L. Brunton, J. L. Proctor, and J. N. Kutz, Inferring biological networks by sparse identification of nonlinear dynamics, IEEE Transactions on Molecular, Biological and Multi-Scale Communications **2**, 52 (2016).

[20] S. H. Rudy, S. L. Brunton, J. L. Proctor, and J. N. Kutz, Data-driven discovery of partial differential equations, Science advances **3**, e1602614 (2017).

[21] P. Zheng, T. Askham, S. L. Brunton, J. N. Kutz, and A. Y. Aravkin, A unified framework for sparse relaxed regularized regression: Sr3, IEEE Access **7**, 1404 (2018).

[22] K. Champion, P. Zheng, A. Y. Aravkin, S. L. Brunton, and J. N. Kutz, A unified sparse optimization framework to learn parsimonious physics-informed models from data, IEEE Access **8**, 169259 (2020).

[23] B. M. De Silva, K. Champion, M. Quade, J.-C. Loiseau, J. N. Kutz, and S. L. Brunton, Pysindy: a python package for the sparse identification of nonlinear dynamics from data, arXiv preprint arXiv:2004.08424 (2020).

[24] A. A. Kaptanoglu, B. M. de Silva, U. Fasel, K. Kaheman, A. J. Goldschmidt, J. L. Callaham, C. B. Delahunt, Z. G. Nicolaou, K. Champion, J.-C. Loiseau, *et al.*, Pysindy: A comprehensive python package for robust sparse system identification, arXiv preprint arXiv:2111.08481 (2021).

[25] S. Sahoo, C. Lampert, and G. Martius, Learning equations for extrapolation and control, in *International Conference on Machine Learning* (PMLR, 2018) pp. 4442–4450.

[26] The Feynman Lectures on Physics (2024), [Online; accessed 7. Nov. 2024].

[27] M. Cranmer, Interpretable machine learning for science with pysis and symbolicregression.jl, arXiv preprint arXiv:2305.01582 (2023).

[28] F. Rothlauf, Representations for genetic and evolutionary algorithms, in *Representations for Genetic and Evolutionary Algorithms* (Springer, 2006) pp. 9–32.

[29] M. Quade, M. Abel, J. Nathan Kutz, and S. L. Brunton, Sparse identification of nonlinear dynamics for rapid model recovery, Chaos: An Interdisciplinary Journal of Nonlinear Science **28**, 063116 (2018).

[30] K. Stanislawska, K. Krawiec, and Z. W. Kundzewicz, Modeling global temperature changes with genetic programming, Computers & Mathematics with Applications **64**, 3717 (2012).

[31] Y. Wang, N. Wagner, and J. M. Rondinelli, Symbolic regression in materials science, MRS Communications **9**, 793 (2019).

[32] Y. Chen, M. T. Angulo, and Y.-Y. Liu, Revealing complex ecological dynamics via symbolic regression, BioEssays **41**, 1900069 (2019).

[33] I. A. Abdellaoui and S. Mehrkanoon, Symbolic regression for scientific discovery: an application to wind speed forecasting, in *2021 IEEE Symposium Series on Computational Intelligence (SSCI)* (IEEE, 2021) pp. 01–08.

[34] J. Luo and C. L. Yu, The application of symbolic regression on identifying implied volatility surface, Mathematics **11**, 2108 (2023).

[35] E. Kiyani, K. Shukla, G. E. Karniadakis, and M. Karttunen, A framework based on symbolic regression coupled with extended physics-informed neural networks for gray-box learning of equations of motion from data, arXiv preprint arXiv:2305.10706 (2023).

[36] J. P. Gudetti, S. J. M. Yazdi, J. Baqersad, D. Peters, and M. Ghamari, *Data-Driven Modeling of Linear and Nonlinear Dynamic Systems for Noise and Vibration Applications*, Tech. Rep. (SAE Technical Paper, 2023).

[37] M. Miyazaki, K.-I. Ishikawa, K. Nakashima, H. Shimizu, T. Takahashi, and N. Takahashi, Application of the symbolic regression program ai-feynman to psychology, Fron-

tiers in Artificial Intelligence **6**, 1039438 (2023).

[38] K. W. Wong and M. Cranmer, Automated discovery of interpretable gravitational-wave population models, arXiv preprint arXiv:2207.12409 (2022).

[39] M. Schmidt and H. Lipson, Eureqa (version 0.98 beta), Nutonian Inc., Boston MA (2014).

[40] W. La Cava, P. Orzechowski, B. Burlacu, F. O. de França, M. Virgolin, Y. Jin, M. Kommenda, and J. H. Moore, Contemporary symbolic regression methods and their relative performance, arXiv preprint arXiv:2107.14351 (2021).

[41] E. N. Lorenz, Deterministic Nonperiodic Flow, *J. Atmos. Sci.* **20**, 130 (1963).

[42] H. Haken and H. Sauermann, Nonlinear interaction of laser modes, *Z. Phys.* **173**, 261 (1963).

[43] B.-W. Shen, Attractor Coexistence, Butterfly Effects, and Chaos (ABC): A Review of Lorenz and Generalized Lorenz Models, in *16th Chaotic Modeling and Simulation International Conference* (Springer, Cham, Switzerland, 2025) pp. 589–610.

[44] É. Diz-Pita and M. V. Otero-Espinar, Predator–Prey Models: A Review of Some Recent Advances, *Mathematics* **9**, 1783 (2021).

[45] P. J. Wangersky, Lotka–volterra population models, *Annual Review of Ecology and Systematics* **9**, 189 (1978).

[46] S. Annas, M. I. Pratama, M. Rifandi, W. Sanusi, and S. Side, Stability analysis and numerical simulation of seir model for pandemic covid-19 spread in indonesia, *Chaos, solitons & fractals* **139**, 110072 (2020).

[47] I. Korolev, Identification and estimation of the seird epidemic model for covid-19, *Journal of econometrics* **220**, 63 (2021).

[48] M. Oke, O. Ogunmiloro, C. Akinwumi, and R. Raji, Mathematical modeling and stability analysis of a sirv epidemic model with non-linear force of infection and treatment, *Communications in Mathematics and Applications* **10**, 717 (2019).

[49] H. Hu, X. Yuan, L. Huang, and C. Huang, Global dynamics of an sirs model with demographics and transfer from infectious to susceptible on heterogeneous networks, *Math. Biosci. Eng.* **16**, 5729 (2019).

[50] W. J. Conover, *Practical Nonparametric Statistics, 3rd Edition* (Wiley, Hoboken, NJ, USA, 1999) p. 350.

[51] L. Breiman, Random forests, *Machine learning* **45**, 5 (2001).

[52] G. Biau and E. Scornet, A random forest guided tour, *Test* **25**, 197 (2016).

[53] S.-M. Udrescu and M. Tegmark, AI-Feynman (2020), [Online; accessed 22. Jul. 2025].

[54] M. Virgolin and S. P. Pissis, Symbolic regression is NP-hard, *Transactions on Machine Learning Research* (2022).

[55] B. Brum and L. Lober, GitHub repository for all code used in this study (2025), [https://github.com/luizalober/review\\_symb\\_regression/](https://github.com/luizalober/review_symb_regression/).